BIOCHEMISTRY

 Volume 46, Number 30 July 31, 2007

Current Topics

PDZ Domains: Folding and Binding†

Per Jemth*,‡ and Stefano Gianni*,§

Department of Medical Biochemistry and Microbiology, Uppsala University, BMC Box 582, SE-75123 Uppsala, Sweden, and Dipartimento di Scienze Biochimiche "A. Rossi Fanelli" and Istituto di Biologia e Patologia Molecolari del CNR, Università di Roma "La Sapienza", Piazzale A. Moro 5, 00185 Rome, Italy

Received May 7, 2007; Revised Manuscript Received June 12, 2007

ABSTRACT: The PDZ domain is one of the most common protein−protein interaction domains in humans, and it is found in all kingdoms of life. We will review recent progress in the understanding of biophysical aspects of PDZ domains with emphasis on the folding and binding reactions. Finally, we discuss an intriguing correlation between stability and binding of peptide for PDZ2 from PTP-BL.

The PDZ[1] domain is a widespread protein module that has been recruited to serve multiple functions during the course of evolution. PDZ domains are thus found in various proteins in humans, alone or in arrays, and in particular they play prominent roles in synapse formation in mammals (*1*). The canonical structure consists of five to six β-strands (β1−β6) and two α-helices (α1, α2) (Figure 1). Most commonly, the C-terminus of the ligand protein binds to a groove in the PDZ domain between β2 and α2 to form a sheet together with strands β2 and β3 from the domain. The PDZ domains have been grouped into different classes based on their ligand preferences (*2*), but this classification only works to a certain extent (*3*). The specificity of PDZ domains toward different peptides has been thoroughly studied (e.g., refs *4*−*7*) and reviewed (*2*). We will not go into detail on this issue but merely conclude that these studies and others (e.g., refs *3* and *8*) suggest that PDZ domains display overlapping specificity and promiscuity toward their different target ligands. Their plasticity in terms of ligand preference is also reflected in studies where PDZ domains were engineered to display new ligand specificities (*6*, *9*, *10*).

Two of the most well studied PDZ domains from a biophysical point of view are PDZ3 from PSD-95 and PDZ2 from PTP-BL (also denoted PTPL1, PTP-BAS, and PTP1E), and these two PDZ domains have been at the focus of attention in our laboratories. We will first describe the folding mechanism of PDZ domains, based on results from our laboratories. We will then discuss the binding reaction of PDZ domains. Finally, we will address the question whether these two events are coupled in any way, i.e., if there are structure−reactivity relationships that apply to both folding and binding.

FOLDING AND STABILITY

A crucial issue when characterizing the folding reaction of any protein lies in identifying a good optical probe. In the case of the PDZ domain family, we successfully tackled this problem by engineering a tryptophan residue in position 43 of PTP-BL PDZ2 (numbering according to NMR structure, PDB code 1GM1) (*11*, *12*). Indeed, with the exception of the nNOS PDZ domain, mutation to Trp at the homologous position of other PDZ domains yielded an excellent

† This work was funded in part by the Swedish Research Council.

* Corresponding authors. P.J.: e-mail, Per.Jemth@imbim.uu.se; phone, +46-18-4714557; fax, +46-18-4714673. S.G.: e-mail, Stefano.Gianni@uniroma1.it; phone, +39-06-49910548.

‡ Uppsala University.

§ Università di Roma "La Sapienza".

[1] Abbreviations: PDZ, *p*ostsynaptic density protein-95, *d*isk-large tumor suppressor protein, *z*onula occludens-1; PTP-BL, protein tyrosine phosphatase-BL; PSD-95, postsynaptic density protein-95.

10.1021/bi7008618 CCC: $37.00
Published on Web 07/10/2007

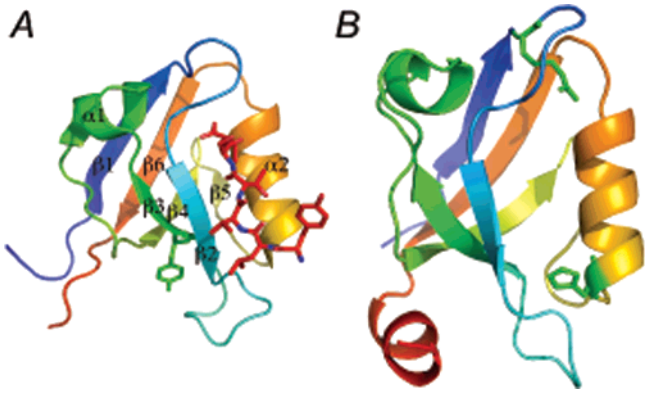

FIGURE 1: 3D structures of (A) PTP-BL PDZ2 solved by NMR (with bound peptide in red) (*38*) and (B) PSD-95 PDZ3 solved by X-ray crystallography (*14*). The structures are rainbow colored from the N-terminus (blue) to the C-terminus (red). In the canonical PDZ−peptide interaction the peptide forms an extended β-sheet with strands β2 and β3 of the PDZ domains. The Tyr highlighted in green in PTP-BL PDZ2 was mutated to a Trp in our studies. This Trp served as a fluorescent probe in folding studies and as a FRET probe in binding studies. Two conserved residues are highlighted in green in PSD-95 PDZ3: Arg318, which governs the salt dependence, and His372, which governs the pH dependence of the binding reaction of this PDZ domain. (The C-terminal helix of PSD-95 PDZ3 is not part of the canonical PDZ structure but was included in our experiments to increase the stability and expression yield.) The structures were drawn in PyMOL (*63*).

probe to study the PDZ folding reaction (*11*−*13*). Isolated PDZ domains typically fold into a well-defined native structure (*14*). The observed thermodynamic stability of PDZ domains, as revealed from equilibrium urea and temperature-induced denaturations, ranges between 3 and 6 kcal mol^{-1} at 25 °C and neutral pH (*11*−*13*, *15*, *16*). This value is consistent with those observed for other small single domain proteins (*17*). Furthermore, different members of the PDZ domain family display a similar degree of denaturation cooperativity, namely, a similar m_{D-N} value of about 1.2 kcal mol^{-1} M^{-1}. The m_{D-N} value relates the free energy of (un)folding ΔG_{D-N} to the denaturant concentration in solvent-induced denaturation experiments (eq 1; cf. ref *18*):

$$\Delta G_{D-N} = \Delta G_{D-N}^{H_2O} - m_{D-N}[\text{denaturant}] \qquad (1)$$

The similar m_{D-N} value among PDZ domains suggests that they have a similar and thus probably low residual structure content in the denatured state.

The folding pathway of PTP-BL PDZ2 has been investigated in detail. Careful investigation of folding and unfolding kinetics of PDZ2 at different pH values revealed the presence of an unfolding intermediate, as detected from the complex dependence of the unfolding kinetics on denaturant concentration (*12*). Quantitative analysis of observed kinetics suggested that the folding of PTP-BL PDZ2 could be satisfactorily described by a three-state mechanism, involving two rate-limiting barriers (namely, a denatured-like TS1 and a native-like TS2) (Figure 2). Further, it was found that the intervening folding intermediate is a high-energy species in the folding pathway of the PDZ domains that never accumulates in the (un)folding reaction and its presence may only be invoked from the observed change in rate-limiting step with increasing denaturant concentration (TS1 and TS2 being rate limiting at low and high denaturant concentration, respectively). Under such conditions, the intermediate is an

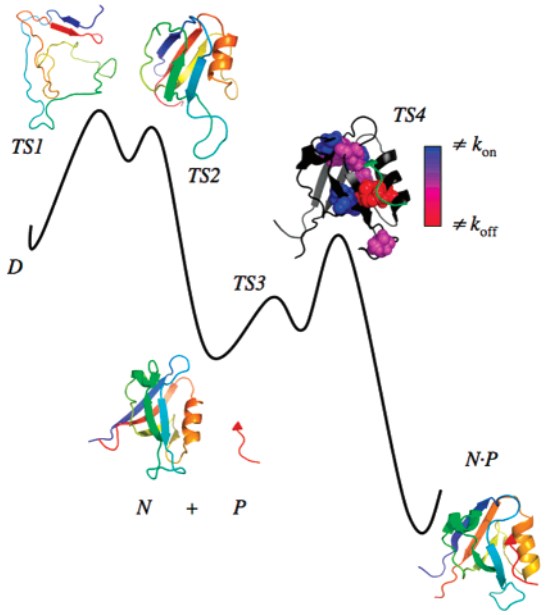

FIGURE 2: Schematic energy diagram showing the folding of PTP-BL PDZ2 followed by binding of a peptide ligand. Depending on the experimental conditions, different transition states (TS1 and TS2) are rate limiting for the folding reaction. Representative computational structures of TS1 and TS2 are shown. The structural properties of TS1 and TS2 as calculated from the whole structure ensemble generated by restrained molecular dynamics simulations are discussed in the text. For the binding reaction available kinetic data are best described with a model where TS4 in the figure is higher in energy than TS3. Owing to the different nature of the protein folding and binding reactions, implying different preexponential factors, the relative free energies of folding and binding transition states cannot be directly compared. The experimental basis for the folding and binding models are described in refs *23* and *38*, respectively.

on-pathway productive and obligatory species in the PDZ folding pathway (*19*, *20*).

The principal aim of protein folding studies lies in dissecting the molecular details of the folding reaction at atomic resolution. In the case of PDZ domains, the presence of two distinct and experimentally accessible transition states allowed us to characterize in detail both the early and late events occurring in the protein folding reaction. However, since transition states never accumulate, information about their structure can only be inferred indirectly. In particular, by systematically mutating residues and probing the effects on folding kinetics and stability, it is possible to map out interaction networks present in the transition states. The strength of the contacts is measured by the Φ value, which normalizes the stability loss of the transition state to that of the native state (*21*). $\Phi = 1$ indicates that the site of mutation is fully structured in the transition state, and $\Phi = 0$ indicates that such a site is as unfolded as the denatured state. Furthermore, experimentally determined Φ values may be employed as restraints in molecular dynamics simulation to calculate the entire structure of folding transition states (*22*).

Representative structures for the two folding transition states, together with a schematic energy diagram for the observed folding reaction, are shown in Figure 2. These structures resulted from a combined experimental (Φ value analysis based on the purification and characterization of 31 site-directed mutants) and theoretical (molecular dynamics simulations) study (*23*). Although the overall topology of

the early transition state (TS1) appears to be very heterogeneous and quite expanded, a specific cluster of strong interresidue interactions in β-strands 1, 4, and 6 could be identified in all of the structures of the ensemble; these interactions include Leu66−Leu95 and Arg64−Glu97 (between β4 and β6) and Asp12−Lys98, Phe14−Leu96, and Val16−Leu94 (between β1 and β6). The presence of this cluster restricts significantly the number of possible conformations of the polypeptide chain committing the structure to a native-like topology. The second transition state (TS2) is more compact and displays a more pronounced native-like topology together with a high degree of secondary structure formation. The overall architecture of TS2 is defined by the presence of stabilizing interactions between residues in β1, β2, β3, β4, and β6 with further supporting interactions involving residues in β1 and α1; these interactions, in addition to those already present in TS1, include Gly26−Ile48 and Ser28−Ala46 (between β2 and β3) and Glu17−Asp56 and Ala19−Glu54 (between β1 and α1).

A quantitative comparison of the kinetic folding pathway of different PDZ domains suggested that this family shares a common folding mechanism (*13*). This observation parallels previous results on the SH3 (*24*, *25*) and cytochrome *c* (*26*) protein families. Indeed, as observed in the case of PTP-BL PDZ2, folding kinetics is characterized by a change in rate-limiting step between TS1 and TS2 with increasing denaturant concentration. In all cases, the denatured-like TS1 was found to be rate limiting in water. More focused studies, based on comparative Φ value analyses, will clarify if also the molecular details of the protein folding reaction are conserved among the different members of the PDZ domain family.

BINDING

The binding strength, or affinity, between a protein and its ligand is given by the equilibrium dissociation constant K_D. In vivo, most K_D values for various protein−ligand interactions range between low nanomolar [for example, in transcription factor−DNA interactions (*27*)] to millimolar [many enzyme−substrate interactions (*18*)], depending on the function of the protein−ligand interaction. For example, in systems, which must respond rapidly to a change in conditions, it is appropriate with a fairly weak protein−protein interaction (K_D in the micromolar to millimolar range) that allows the complex to dissociate within seconds or fractions of a second (high dissociation rate constant, k_{off}). The equilibrium dissociation constants for PDZ domains and peptides mimicking the C-termini of their ligands are normally in the 1−50 μM range as judged by in-solution assays, both by fluorometric methods (*8*, *28*−*34*) and microcalorimetry (*7*, *16*, *35*, *36*). Microcalorimetric studies on PTP-BL PDZ2 (*36*) and PSD-95 PDZ3 (*7*) with peptides corresponding to native ligands show that the main contribution to the binding free energy ΔG comes from the enthalpy ΔH. The contribution from the entropy of binding ($T\Delta S$) is less and could both increase and reduce the affinity, depending on temperature and ligand. We have measured binding kinetics for the interaction of PSD-95 PDZ3 or PTP-BL PDZ2 with their respective ligand peptides using stopped-flow spectrofluorometry (*29*, *37*, *38*). The association rate constants k_{on} (10^6−10^7 M^{-1} s^{-1}) and dissociation rate constants (1−10 s^{-1}) at 10 °C and neutral pH yielded equilibrium dissociation constants (k_{off}/k_{on}) in the same range as those obtained from the studies at equilibrium. There are some conflicting results regarding the rate constants for the binding kinetics of PDZ−peptide interactions. Studies on PTP-BL PDZ2 using surface plasmon resonance (*39*) yielded much higher affinities, in the nanomolar range, as compared to those estimated by NMR (*40*), time-resolved fluorometry (*29*, *38*), and microcalorimetry (*36*). Also, the interactions of PTP-BL PDZ3 and mDlg PDZ2 with their respective ligands were found to be in the nanomolar range by surface plasmon resonance (*5*). In these cases (*5*, *39*) the determined association rate constants were approximately 10−100-fold lower and the dissociation rate constants 1000−10000-fold lower than rate constants measured by stopped-flow and continuous-flow methods (*29*, *37*, *38*). The reason for these differences is unclear, but the agreement between the fluorometric and microcalorimetric data suggests that rate constants from stopped-flow measurements are accurate.

The medium-range affinity of PDZ domains toward their target ligands, as measured by microcalorimetry and change of fluorescence in in-solution studies, is in line with the observed promiscuity of PDZ−ligand interactions (*8*). However, one should bear in mind that few studies have assessed the affinity between PDZ domains and full-length target proteins, where potential interactions outside the ligand-binding pocket might contribute binding energy and increase the affinity (*41*, *42*). One example of a study where a more native-like PDZ ligand was used is the binding reaction between PSD-95 PDZ2 and nNOS PDZ. Here, a β-finger of nNOS PDZ interacts with the peptide-binding pocket of PSD-95 PDZ2 in a noncanonical manner, in the sense that there is no C-terminal carboxylate involved in the interaction (*43*, *44*). The affinity between PSD-95 PDZ2 and nNOS PDZ was estimated by surface plasmon resonance to be 0.12 μM (*45*).

Both PTP-BL PDZ2 and PSD-95 PDZ3 display so-called class I specificity toward target ligands, where the three last residues of the peptide ligand are S/T-X-Φ-COO^- (*2*). X is any residue and Φ is a hydrophobic residue; for example, for PTP-BL PDZ2 and PSD-95 PDZ3 a valine is preferred at the C-terminus. The preference for a serine or threonine residue at position −2 stems from a conserved histidine in helix α2 of the PDZ domain. This histidine makes a hydrogen bond with the hydroxyl group of the serine or threonine (*14*) and is important for the affinity toward the peptide [$\Delta\Delta G$ for the His → Ala mutation is 2.5−3 kcal mol^{-1} (*37*)]. The pH dependence of the affinity between PSD-95 PDZ3 and peptide was shown to be due to protonation of this conserved histidine below pH 7 (*37*). In the same work a conserved positively charged residue (Arg318 in PSD-95 PDZ3) at the end of β1 was found to be responsible for the salt dependence of the affinity for PSD-95 PDZ3. Interestingly, this residue interacts with the carboxylate of the peptide ligand via a water molecule and is not making a direct salt bridge (*14*). The effect of salt on the binding reaction is on the association rate constant, probably not due to screening of long-range interactions but to direct binding of the chloride ion to the arginine. The chloride ion thus functions as a competitive inhibitor and blocks access of the peptide to the binding pocket (*37*). It is however not clear whether this residue governs the salt dependence of other PDZ−ligand interactions since mutation

of the corresponding residue in α1-syntrophin PDZ (Lys → Met) did not abolish the effect of NaCl on the equilibrium dissociation constant (*15*).

To detect possible faster events on the binding reaction pathway, we employed continuous-flow fluorometry and found, at least for PTP-BL PDZ2, that a one-step mechanism is too simple to describe the data. In a one-step mechanism (Scheme 1) under pseudo-first-order conditions ([B] ≫ [A]) the observed rate constant k_{obs} is a linear function of the microscopic rate constants k_{on} and k_{off} (eq 2).

Scheme 1

$$A + B \rightleftharpoons AB$$

$$k_{obs} = k_{on}[B] + k_{off} \quad (2)$$

For the reaction between PTP-BL PDZ2 and its target peptide, k_{obs} was linear with both increasing [peptide] and [PDZ2] under conditions where the stopped-flow technique could be used (*29*). But, measurements with the continuous-flow fluorometer demonstrated that k_{obs} values deviate from linearity at high observed rate constants resulting in a hyperbolic dependence of k_{obs} versus [peptide] or [PDZ2] (*38*). Such behavior reflects a change in the kinetics, from a second-order event (association of PDZ and peptide) to a first-order event (conformational change; see Schemes 2 and 3).

Scheme 2

$$A + B \rightleftharpoons AB \rightleftharpoons A^*B$$

Scheme 3

$$A + B \rightleftharpoons A^* + B \rightleftharpoons A^*B$$

Importantly, varying the concentration of peptide at constant [PDZ] and varying the concentration of PDZ at constant [peptide] yielded identical k_{obs} values. This symmetry with regard to the varied species is consistent with a two-step induced fit mechanism (*46*) (Scheme 2). In such a mechanism, the conformational change occurs subsequent to the association of protein and ligand. In many cases this mechanism is difficult to distinguish from a fast preequilibrium model (Scheme 3), and the term "induced fit" is often used although the actual order of events has not been experimentally demonstrated. While kinetics can unambiguously identify the presence of a conformational change event, it is difficult to define whether the PDZ domain, the peptide, or both experience such monomolecular step. In the case of PTP-BL PDZ2 experimental evidence from NMR and protein engineering suggests that the observed kinetic barrier results from a conformational transition in the PDZ domain (*38*) (see section Conserved Networks of Interacting Residues in PDZ Domains). The complete pathway for folding and binding for PTP-BL PDZ2 is pictured schematically in an energy diagram in Figure 2. Is a conformational change upon ligand binding a general property of PDZ domains? The fast binding kinetics of PSD-95 PDZ3 displayed a slight deviation from linearity at high PDZ3 concentrations, but neither structural data (*14*) nor mutagenesis of core residues (*38*) provided additional evidence for a second step in the binding reaction of PSD-95 PDZ3. Finally, the slope of the temperature dependence of ΔH for binding (ΔC_p), as determined by microcalorimetry, is also consistent with a lock-and-key mechanism of this PDZ domain (*7*).

There are however at least two more examples of structural transitions upon ligand binding in PDZ domains. Grembecka et al. (*47*) found that the peptide-binding pocket of syntenin PDZ2 (*3*) can undergo conformational changes involving the α2 helix to accommodate different side chains of the ligand peptide at positions 0 and −2. Peterson et al. (*48*) demonstrated that the Rho GTPase Cdc42 binds to a CRIB domain of the protein Par-6. The CRIB domain sits adjacent to a PDZ domain, and binding of Cdc42 induces a conformational change in the PDZ domain that leads to a roughly 13-fold increase in affinity for the PDZ domain toward its target ligand.

CONSERVED NETWORKS OF INTERACTING RESIDUES IN PDZ DOMAINS

One important issue in protein chemistry is allostery within single domains and implications for the function of the protein; in particular, do the dynamics inherent in proteins translate into functional allostery (*49*)? The PDZ domain scaffold has been used in computational studies to assess the significance of evolutionarily conserved networks of interacting residues (*50*−*52*). The idea is that networks important for function should be conserved during evolution, in the same way as crucial residues are conserved. Mutation of one residue in the network should therefore be reflected in other mutations in the network that would compensate for possible loss of function from the first mutation. Is there any experimental evidence that such statistical coupling determined from sequence alignments is functionally relevant, in terms of the binding reaction? In the original paper by Lockless and Ranganathan (*51*) dissociation constants for PSD-95 PDZ3 and a target peptide were determined in conjunction with double mutant cycles. The mutations used to test whether the statistical coupling was associated with energetic coupling were however nonconservative (for example, Phe → Lys) and the measured coupling energies low [0−1.5 kT for most positions, i.e., roughly 0−1 kcal mol^{-1}, which might be within the error of the measurement (cf. refs *21*, *53*, and *54*)]. Nevertheless, the experimental data agreed well with their theoretical predictions, suggesting that the evolutionarily conserved network found in PDZ domains actually is working as an energetically coupled network in PSD-95 PDZ3. Using fast kinetics and protein engineering, we found little evidence for a conformational transition in PSD-95 PDZ3 which could be associated with a functional allosteric network (*38*). Two of the residues in the network were mutated [Val362 → Ala and Val386 → Ala; numbering according to Doyle et al. (*14*)], but the binding kinetics were virtually identical to those of the wild-type PSD-95 PDZ3. Energetic coupling between residues may be related to the dynamics of a protein as measured by NMR. Human PTP-BL PDZ2 has been subjected to NMR studies that addressed the dynamics of the domain (*28*, *55*) and the correlation of dynamics with the evolutionarily conserved network of PDZ domains (*51*). Long-range dynamic effects were indeed detected by NMR (*55*). Two regions of the PDZ domain, referred to as distal surface 1 and 2, respectively, contained methyl groups that displayed changes in the two parameters, τ_e (internal correlation time) and S^2_{axis} (generalized squared order parameter), upon binding of ligand, demonstrating that

the dynamics of the protein is modulated by interaction with the ligand and not only in the ligand-binding pocket. Moreover, the change in dynamics of PTP-BL PDZ2 (*55*) correlated well with the evolutionarily conserved communication pathway, or network, found by Lockless and Ranganathan (*51*). Is this network used in allosteric transmission in PTP-BL PDZ2, i.e., is it working as an energetic communication pathway? Fuentes et al. went on to investigate the coupling network by mutagenesis in combination with studies on binding affinity and dynamics (*28*). Most mutations had a limited effect on K_D (1−2-fold) and the side-chain dynamics, but one mutation involving a network residue, Ile27 → Phe [numbering according to the NMR structure of mouse PTP-BL PDZ2, PDB codes 1GM1 and 1VJ6 (*38*, *40*)], caused large changes in side-chain dynamics and was considered a hub in the transmission of changes in dynamics in the protein core. However, no energetic coupling between Ile27 and the His76 was present as shown by a double mutant cycle; His76 forms a hydrogen bond with the hydroxyl group of residue −2 in the peptide and is a highly conserved residue that "defines" the statistical network. These two residues coupled energetically with one another in PSD-95 PDZ3 as probed by double mutant cycles (using non-conservative mutations) (*51*). In our work on the mouse PTP-BL PDZ2 (approximately 94% identical to the human one) we found evidence for a conformational change upon binding of PTP-BL to target peptide. First, the NMR structure of the peptide-bound PDZ domain (*38*) was different from that of the unliganded protein (*40*, *56*). Second, several conservative mutations (i.e., Ile → Val or Ala, Val → Ala, Ala → Gly) of hydrophobic residues in the core of PTP-BL PDZ2 modulated the association rate constant k_{on} for the PDZ−peptide interaction, demonstrating the presence of long-range interactions in the core. Third, the previously described kinetics of binding follow an induced fit mechanism. Our data are thus consistent with a network of interacting residues in PTP-BL PDZ2 that could act as a communication network between distal parts of the molecule (allostery). But, it is important to point out that the conformational change observed by kinetics might be unrelated to the conformational change detected by NMR and the effects of mutation on association rate constants and, of course, to the evolutionarily conserved network of interacting residues found in PDZ domains (*50*, *51*). Three of the residues in the proposed network were mutated, Ile27 → Val, Val68 → Ala, and Val92 → Ala, and the mutants were subjected to stopped-flow binding experiments. The association rate constants were decreased by a factor of 2 for the Val68 → Ala and Val92 → Ala mutants but remained constant for the Ile27 → Val mutant. Other mutations in the core involving residues that are not part of the conserved network yielded similar results. In conclusion, the work by Fuentes et al. on human PTP-BL PDZ2 (*28*) and by us on mouse PTP-BL PDZ2 (*38*) suggests that the evolutionarily conserved network does not serve as an energetic network in this PDZ domain.

STABILITY AND ALLOSTERY: TWO SIDES OF THE SAME COIN?

One of the central problems in structural biology lies in defining the role of dynamics and stability in protein function: the dynamics of a protein may for example be coupled to catalysis (*57*) or binding (*58*−*60*). Taking it to the extreme, in the case of intrinsically unstructured proteins (*61*), a binding reaction may induce the folding of a protein, protein folding being the most radical example of protein dynamics. However, even proteins displaying a well-defined native state, such as the PDZ domains considered here, may in theory be dependent on their stability and dynamics to exert their function. We produced several mutants of PTP-BL PDZ2 and subjected them to both folding (*12*, *23*) and binding studies (*29*, *38*). Thus, available data give us the unique opportunity to evaluate if residues important for the folding reaction of this domain are also important for its function.

Understanding the relationship between two different events or variables often requires cross-correlation plots. A cross-correlation plot is based on the principle that, when and if two events are mutually related, their response to an external perturbation, such as mutagenesis, should be correlated. Figure 3 is a plot of $\Delta\Delta G$ upon mutation for parameters related to the binding reaction (k_{on}, k_{off}, K_D) versus $\Delta\Delta G$ on mutation for PDZ stability and folding rate constant (as given by the unfolding rate constant k_u), respectively. Importantly, we have only included truly distal residues that do not interact directly with the peptide (e.g., all residues in $\alpha 2$ and $\beta 2$ were excluded), and only fully native mutants were considered (i.e., in all cases, the fractional population of native state was >0.96). Interestingly, as shown in Figure 3, available data seem to display a correlation between the energetic barrier for binding, TS4, as given by k_{on}, versus the stability of the mutant ($R = 0.71$) and folding rate constant ($R = 0.65$) (see Figure 2). Such a correlation is not observed for the dissociation rate constant k_{off}, displaying correlation coefficients of 0.4 and 0.2, respectively. Furthermore, we observed slightly decreasing correlation coefficients when the $\Delta\Delta G$'s on mutation from association rate constants were plotted versus native to denatured ($R = 0.71$), native to TS1 ($R = 0.65$) or native to TS2 ($R = 0.60$) stabilities, respectively. Since we have shown previously that a decreasing correlation coefficient may be observed when the stabilities of TS1 and TS2 are plotted versus the native state (*23*), it is likely that the binding event is genuinely correlated with native stability, and the correlations with other folding parameters (e.g., TS1 stability) may simply arise from the intrinsic properties of the folding reaction.

As described above, all of the PDZ domains considered here (including site-directed mutants) fold into a well-defined native state. Hence, a rational explanation of the observed correlation is not obvious. Wolynes and co-workers proposed an interesting mechanism that would account for a correlation between protein stability and binding rates, the fly-casting mechanism (*62*). According to this formalism, protein−substrate binding may involve the formation of a transiently occurring intermediate in which the protein displays a partially folded conformation. The increased capture radius of an expanded state may improve the binding reaction, and an increased binding rate should be observed for destabilized mutants. In the case of the PDZ domain family, while we observed a correlation between association rate constants and protein stability, the binding rate constants seem to increase with increasing stability. This observation suggests that, on the contrary to what would be expected from the fly-casting mechanism, binding is here coupled with a rate-limiting compaction event.

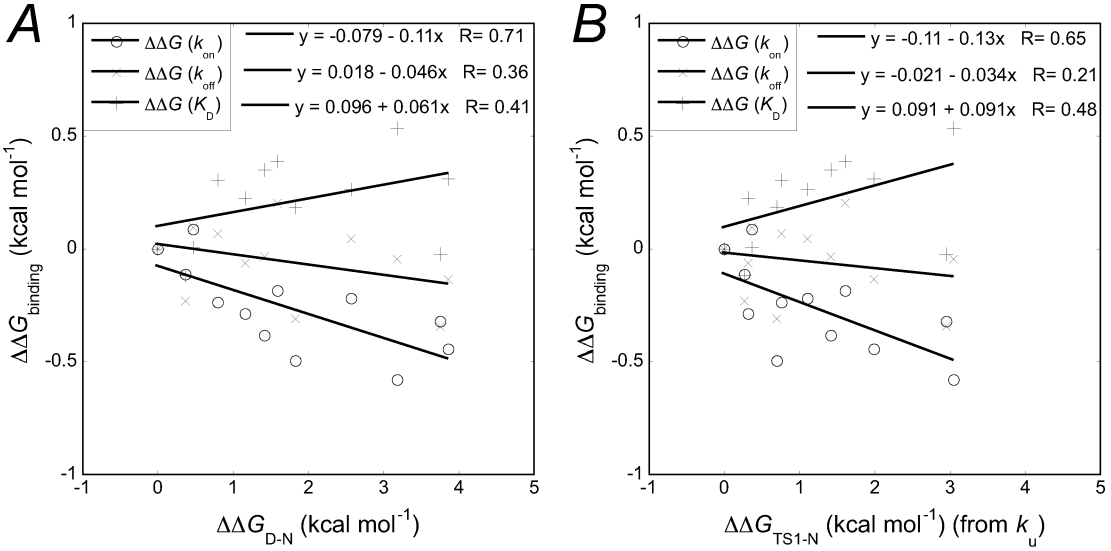

FIGURE 3: Cross-correlations between the free energy of binding parameters (k_{on}, k_{off}, K_D) and (A) the stability of the mutant and (B) the free energy between TS1 and the native state for a number of core mutants of PTP-BL PDZ2. Residues from α2 and β2 were excluded. Thus, none of these mutations involve residues that interact directly with the peptide ligand. The mutants included in the plot are pseudo-wild type (Y43W), L18A, I42V, V44A, A46G, A52G, A53G, I59V, V65A, L66A, V68A, and V92A. Binding rate constants used to calculate $\Delta\Delta G$ ($=\Delta G^{\text{mutant}} - \Delta G^{\text{wild type}}$) for k_{on}, k_{off}, and K_D were from ref *38* except for I42V (previously unpublished). The change in stability on mutation, $\Delta\Delta G_{D-N}$ ($=\Delta G_{D-N}{}^{\text{wild type}} - \Delta G_{D-N}{}^{\text{mutant}}$), and change in stability of TS1 on mutation, $\Delta\Delta G_{TS1-N}$ [$=\Delta G_{TS1-N}{}^{\text{wild type}} - \Delta G_{TS1-N}{}^{\text{mutant}} = RT \ln(k_{u1}{}^{\text{mutant}}/k_{u1}{}^{\text{wild type}})$], are previously unpublished raw data that were used to calculate (published) Φ values for TS1 in ref *23*.

On the basis of the observed correlation, an interesting pathway for PDZ allostery may be invoked: it appears that the network of residues driving the conformational change superposes with those influencing folding and stability of the protein. Indeed, since the mutations far from the binding site that destabilize the native state also destabilize the rate-limiting barrier for the association reaction, it appears that TS4 represents a more compact version of the native state. Hence, it is tempting to speculate that the early events in allosteric communication pathways involve a global compaction of the polypeptide chain with non-native interactions in TS4 (see Figure 2). Downhill of the main energy barrier TS4, a local rearrangement of the actual binding site occurs, which locks the short-range interactions between peptide and protein in place. This mechanism is also supported by the observation that mutations in the PDZ binding site, even when involving positions whose side chains are not in direct contact with the peptide ligand, mainly affect the dissociation rate constant, as mirrored by the mutants V29A and A81G, located in β2 and α2, respectively.

CONCLUSIONS

PDZ domains are fairly stable protein−protein interaction domains that bind ligands with micromolar affinity. The observed dissociation constants are consistent with their role as malleable protein−protein interaction modules, which can bind to and dissociate from their target ligands on a fast time scale. Structural and biophysical characterization of some PDZ domains, such as PTP-BL PDZ2 and syntenin PDZ, suggests that binding involves a conformational change in the PDZ domain comprising small rearrangements of several core residues and the orientation of helix α2. Intriguingly, in PTP-BL PDZ2 there is a correlation between thermodynamic folding stability (as probed by the change in free energy between the native and the denatured state) and the energetics of ligand binding, suggesting that common features may be invoked for the molecular pathways of stability and binding. One plausible mechanism for PTP-BL PDZ2 allostery is a global compaction of the polypeptide chain after the encounter of the target ligand, followed by a local rearrangement of the binding site. Future work will highlight the generality of this mechanism in protein−ligand interactions.

ACKNOWLEDGMENT

We thank members of our laboratories for stimulating discussions.

REFERENCES

1. Kim, E., and Sheng, M. (2004) PDZ domain proteins of synapses, *Nat. Rev. Neurosci. 5*, 771−781.
2. Hung, A. Y., and Sheng, M. (2002) PDZ domains: structural modules for protein complex assembly, *J. Biol. Chem. 277*, 5699−5702.
3. Kang, B. S., Cooper, D. R., Devedjiev, Y., Derewenda, U., and Derewenda, Z. S. (2003) Molecular roots of degenerate specificity in syntenin's PDZ2 domain: reassessment of the PDZ recognition paradigm, *Structure 11*, 845−853.
4. Skelton, N. J., Koehler, M. F. T., Zobel, K., Wong, W. L., Yeh, S., Pisabarro, M. T., Yin, J. P., Lasky, L. A., and Sidhu, S. S. (2003) Origins of PDZ domain ligand specificity. Structure determination and mutagenesis of the erbin PDZ domain, *J. Biol. Chem. 278*, 7645−7654.
5. Songyang, Z., Fanning, A. S., Fu, C., Xu, J., Marfatia, S. M., Chishti, A. H., Crompton, A., Chan, A. C., Anderson, J. M., and Cantley, L. C. (1997) Recognition of unique carboxyl-terminal motifs by distinct PDZ domains, *Science 275*, 73−77.
6. Wiedemann, U., Boisguerin, P., Leben, R., Leitner, D., Krause, G., Moelling, K., Volkmer-Engert, R., and Oschkinat, H. (2004) Quantification of PDZ domain specificity, prediction of ligand affinity and rational design of super-binding peptides, *J. Mol. Biol. 343*, 703−718.
7. Saro, D., Li, T., Rupasinghe, C., Paredes, A., Caspers, N., and Spaller, M. R. (2007) A thermodynamic ligand binding study of the third PDZ domain (PDZ3) from the mammalian neuronal protein PSD-95, *Biochemistry 46*, 6340−6352.

8. Lim, I. A., Hall, D. D., and Hell, J. W. (2002) Selectivity and promiscuity of the first and second PDZ domains of PSD-95 and synapse-associated protein 102, *J. Biol. Chem. 277*, 21697−21711.
9. Ferrer, M., Maiolo, J., Kratz, P., Jackowski, J. L., Murphy, D. J., Delagrave, S., and Inglese, J. (2005) Directed evolution of PDZ variants to generate high-affinity detection reagents, *Protein Eng. Des. Sel. 18*, 165−173.
10. Reina, J., Lacroix, E., Hobson, S. D., Fernandez-Ballester, G., Rybin, V., Schwab, M. S., Serrano, L., and Gonzalez, C. (2002) Computer-aided design of a PDZ domain to recognize new target sequences, *Nat. Struct. Biol. 9*, 621−627.
11. Feng, H., Vu, N. D., and Bai, Y. (2005) Detection of a hidden folding intermediate of the third domain of PDZ, *J. Mol. Biol. 346*, 345−353.
12. Gianni, S., Calosci, N., Aelen, J., Vuister, G. W., Brunori, M., and Travaglini-Allocatelli, C. (2005) Kinetic folding mechanism of PDZ2 from PTP-BL, *Protein Eng. Des. Sel. 18*, 389−395.
13. Chi, C. N., Gianni, S., Calosci, N., Travaglini-Allocatelli, C., Engström, Å., and Jemth, P. (2007) A conserved folding mechanism for PDZ domains, *FEBS Lett. 581*, 1109−1113.
14. Doyle, D. A., Lee, A., Lewis, J., Kim, E., Sheng, M., and MacKinnon, R. (1996) Crystal structures of a complexed and peptide-free membrane protein-binding domain: molecular basis of peptide recognition by PDZ, *Cell 85*, 1067−1076.
15. Harris, B. Z., Lau, F. W., Fujii, N., Guy, R. K., and Lim, W. A. (2003) Role of electrostatic interactions in PDZ domain ligand recognition, *Biochemistry 42*, 2797−2805.
16. Kang, B. S., Cooper, D. R., Jelen, F., Devedjiev, Y., Derewenda, U., Dauter, Z., Otlewski, J., and Derewenda, Z. S. (2003) PDZ tandem of human syntenin: crystal structure and functional properties, *Structure 11*, 459−468.
17. Jackson, S. E. (1998) How do small single-domain proteins fold?, *Folding Des. 3*, R81−R91.
18. Fersht, A. (1999) *Structure and Mechanism in Protein Science*, W. H. Freeman, New York.
19. Fersht, A. R. (2000) A kinetically significant intermediate in the folding of barnase, *Proc. Natl. Acad. Sci. U.S.A. 97*, 14121−14126.
20. Ivarsson, Y., Travaglini-Allocatelli, C., Jemth, P., Malatesta, F., Brunori, M., and Gianni, S. (2007) An on-pathway intermediate in the folding of a PDZ domain, *J. Biol. Chem. 282*, 8568−8572.
21. Fersht, A. R., Matouschek, A., and Serrano, L. (1992) The folding of an enzyme. I. Theory of protein engineering analysis of stability and pathway of protein folding, *J. Mol. Biol. 224*, 771−782.
22. Vendruscolo, M., Paci, E., Dobson, C. M., and Karplus, M. (2001) Three key residues form a critical contact network in a protein folding transition state, *Nature 409*, 641−645.
23. Gianni, S., Geierhaas, C. D., Calosci, N., Jemth, P., Vuister, G. W., Travaglini-Allocatelli, C., Vendruscolo, M., and Brunori, M. (2007) A PDZ domain recapitulates a unifying mechanism for protein folding, *Proc. Natl. Acad. Sci. U.S.A. 104*, 128−133.
24. Martinez, J. C., and Serrano, L. (1999) The folding transition state between SH3 domains is conformationally restricted and evolutionarily conserved, *Nat. Struct. Biol. 6*, 1010−1016.
25. Riddle, D. S., Grantcharova, V. P., Santiago, J. V., Alm, E., Ruczinski, I., and Baker, D. (1999) Experiment and theory highlight role of native state topology in SH3 folding, *Nat. Struct. Biol. 6*, 1016−1024.
26. Travaglini-Allocatelli, C., Gianni, S., and Brunori, M. (2004) A common folding mechanism in the cytochrome *c* family, *Trends Biochem. Sci. 29*, 535−541.
27. Maerkl, S. J., and Quake, S. R. (2007) A systems approach to measuring the binding energy landscapes of transcription factors, *Science 315*, 233−237.
28. Fuentes, E. J., Gilmore, S. A., Mauldin, R. V., and Lee, A. L. (2006) Evaluation of energetic and dynamic coupling networks in a PDZ domain protein, *J. Mol. Biol. 364*, 337−351.
29. Gianni, S., Engström, Å., Larsson, M., Calosci, N., Malatesta, F., Eklund, L., Ngang, C. C., Travaglini-Allocatelli, C., and Jemth, P. (2005) The kinetics of PDZ domain-ligand interactions and implications for the binding mechanism, *J. Biol. Chem. 280*, 34805−34812.
30. Harris, B. Z., Hillier, B. J., and Lim, W. A. (2001) Energetic determinants of internal motif recognition by PDZ domains, *Biochemistry 40*, 5921−5930.
31. Long, J. F., Tochio, H., Wang, P., Fan, J. S., Sala, C., Niethammer, M., Sheng, M., and Zhang, M. (2003) Supramodular structure and synergistic target binding of the N-terminal tandem PDZ domains of PSD-95, *J. Mol. Biol. 327*, 203−214.
32. Madsen, K. L., Beuming, T., Niv, M. Y., Chang, C. W., Dev, K. K., Weinstein, H., and Gether, U. (2005) Molecular determinants for the complex binding specificity of the PDZ domain in PICK1, *J. Biol. Chem. 280*, 20539−20548.
33. Piserchio, A., Pellegrini, M., Mehta, S., Blackman, S. M., Garcia, E. P., Marshall, J., and Mierke, D. F. (2002) The PDZ1 domain of SAP90. Characterization of structure and binding, *J. Biol. Chem. 277*, 6967−6973.
34. Novak, K. A. P., Fujii, N., and Guy, R. K. (2002) Investigation of the PDZ domain ligand binding site using chemically modified peptides, *Bioorg. Med. Chem. Lett. 12*, 2471−2474.
35. Saro, D., Klosi, E., Paredes, A., and Spaller, M. R. (2004) Thermodynamic analysis of a hydrophobic binding site: probing the PDZ domain with nonproteinogenic peptide ligands, *Org. Lett. 6*, 3429−3432.
36. Milev, S., Bjelic, S., Georgiev, O., and Jelesarov, I. (2007) Energetics of peptide recognition by the second PDZ domain of human protein tyrosine phosphatase 1E, *Biochemistry 46*, 1064−1078.
37. Chi, C. N., Engström, Å., Gianni, S., Larsson, M., and Jemth, P. (2006) Two conserved residues govern the salt and pH dependencies of the binding reaction of a PDZ domain, *J. Biol. Chem. 281*, 36811−36818.
38. Gianni, S., Walma, T., Arcovito, A., Calosci, N., Bellelli, A., Engström, Å., Travaglini-Allocatelli, C., Brunori, M., Jemth, P., and Vuister, G. W. (2006) Demonstration of long-range interactions in a PDZ domain by NMR, kinetics and protein engineering, *Structure 14*, 1801−1809.
39. Erdmann, K. S., Kuhlmann, J., Lessmann, V., Herrmann, L., Eulenburg, V., Muller, O., and Heumann, R. (2000) The adenomatous polyposis coli-protein (APC) interacts with the protein tyrosine phosphatase PTP-BL via an alternatively spliced PDZ domain, *Oncogene 19*, 3894−3901.
40. Walma, T., Spronk, C. A., Tessari, M., Aelen, J., Schepens, J., Hendriks, W., and Vuister, G. W. (2002) Structure, dynamics and binding characteristics of the second PDZ domain of PTP-BL, *J. Mol. Biol. 316*, 1101−1110.
41. Larsson, M., Hjalm, G., Sakwe, A. M., Engström, A., Höglund, A. S., Larsson, E., Robinson, R. C., Sundberg, C., and Rask, L. (2003) Selective interaction of megalin with postsynaptic density-95 (PSD-95)-like membrane-associated guanylate kinase (MAGUK) proteins, *Biochem. J. 373*, 381−391.
42. Pegan, S., Tan, J., Huang, A., Slesinger, P. A., Riek, R., and Choe, S. (2007) NMR studies of interactions between C-terminal tail of Kir2.1 channel and PDZ1,2 domains of PSD95, *Biochemistry 46*, 5315−5322.
43. Hillier, B. J., Christopherson, K. S., Prehoda, K. E., Bredt, D. S., and Lim, W. A. (1999) Unexpected modes of PDZ domain scaffolding revealed by structure of nNOS-syntrophin complex, *Science 284*, 812−815.
44. Tochio, H., Zhang, Q., Mandal, P., Li, M., and Zhang, M. (1999) Solution structure of the extended neuronal nitric oxide synthase PDZ domain complexed with an associated peptide, *Nat. Struct. Biol. 6*, 417−421.
45. Tochio, H., Mok, Y. K., Zhang, Q., Kan, H. M., Bredt, D. S., and Zhang, M. (2000) Formation of nNOS/PSD-95 PDZ dimer requires a preformed beta-finger structure from the nNOS PDZ domain, *J. Mol. Biol. 303*, 359−370.
46. Olson, S. T., Srinivasan, K. R., Bjork, I., and Shore, J. D. (1981) Binding of high affinity heparin to antithrombin III. Stopped-flow kinetic studies of the binding interaction, *J. Biol. Chem. 256*, 11073−11079.
47. Grembecka, J., Cierpicki, T., Devedjiev, Y., Derewenda, U., Kang, B. S., Bushweller, J. H., and Derewenda, Z. S. (2006) The binding of the PDZ tandem of syntenin to target proteins, *Biochemistry 45*, 3674−3683.
48. Peterson, F. C., Penkert, R. R., Volkman, B. F., and Prehoda, K. E. (2004) Cdc42 regulates the Par-6 PDZ domain through an allosteric CRIB-PDZ transition, *Mol. Cell 13*, 665−676.
49. Gunasekaran, K., Ma, B., and Nussinov, R. (2004) Is allostery an intrinsic property of all dynamic proteins?, *Proteins 57*, 433−443.
50. Dima, R. I., and Thirumalai, D. (2006) Determination of network of residues that regulate allostery in protein families using sequence analysis, *Protein Sci. 15*, 258−268.
51. Lockless, S. W., and Ranganathan, R. (1999) Evolutionary conserved pathways of energetic connectivity in protein families, *Science 286*, 295−299.

52. Suel, G. M., Lockless, S. W., Wall, M. A., and Ranganathan, R. (2003) Evolutionarily conserved networks of residues mediate allosteric communication in proteins, *Nat. Struct. Biol. 10*, 59−69.
53. Fersht, A. R., and Sato, S. (2004) Phi-value analysis and the nature of protein-folding transition states, *Proc. Natl. Acad. Sci. U.S.A. 101*, 7976−7981.
54. Schreiber, G., and Fersht, A. R. (1995) Energetics of protein-protein interactions: analysis of the barnase-barstar interface by single mutations and double mutant cycles, *J. Mol. Biol. 248*, 478−486.
55. Fuentes, E. J., Der, C. J., and Lee, A. L. (2004) Ligand-dependent dynamics and intramolecular signaling in a PDZ domain, *J. Mol. Biol. 335*, 1105−1115.
56. Walma, T., Aelen, J., Nabuurs, S. B., Oostendorp, M., van den Berk, L., Hendriks, W., and Vuister, G. W. (2004) A closed binding pocket and global destabilization modify the binding properties of an alternatively spliced form of the second PDZ domain of PTP-BL, *Structure 12*, 11−20.
57. Eisenmesser, E. Z., Bosco, D. A., Akke, M., and Kern, D. (2002) Enzyme dynamics during catalysis, *Science 295*, 1520−1523.
58. Khajehpour, M., Wu, L., Liu, S., Zhadin, N., Zhang, Z. Y., and Callender, R. (2007) Loop dynamics and ligand binding kinetics in the reaction catalyzed by the *Yersinia* protein tyrosine phosphatase, *Biochemistry 46*, 4370−4378.
59. Lee, A. L., Kinnear, S. A., and Wand, A. J. (2000) Redistribution and loss of side chain entropy upon formation of a calmodulin-peptide complex, *Nat. Struct. Biol. 7*, 72−77.
60. Peng, T., Zintsmaster, J. S., Namanja, A. T., and Peng, J. W. (2007) Sequence-specific dynamics modulate recognition specificity in WW domains, *Nat. Struct. Mol. Biol. 14*, 325−331.
61. Dyson, H. J., and Wright, P. E. (2005) Intrinsically unstructured proteins and their functions, *Nat. Rev. Mol. Cell Biol. 6*, 197−208.
62. Shoemaker, B. A., Portman, J. J., and Wolynes, P. G. (2000) Speeding molecular recognition by using the folding funnel: the fly-casting mechanism, *Proc. Natl. Acad. Sci. U.S.A. 97*, 8868−8873.
63. DeLano, W. L. (2002) The PyMOL Molecular Graphics System, DeLano Scientific, San Carlos, CA.

BI7008618